Published online 16 November 2017

Nucleic Acids Research, 2018, Vol. 46, No. 2 ***897–904***
doi: 10.1093/nar/gkx1136

Structural rearrangements in mRNA upon its binding to human 80S ribosomes revealed by EPR spectroscopy

Alexey A. Malygin[1,2], Dmitri M. Graifer[1,2], Maria I. Meschaninova[1], Alya G. Venyaminova[1], Ivan O. Timofeev[2,3,4], Andrey A. Kuzhelev[2,3,4], Olesya A. Krumkacheva[2,3,4], Matvey V. Fedin[2,3,*], Galina G. Karpova[1,2,*] and Elena G. Bagryanskaya[2,4,*]

[1]Institute of Chemical Biology and Fundamental Medicine SB RAS, pr. Lavrentjeva 8, Novosibirsk 630090, Russia, [2]Novosibirsk State University, Pirogova Str. 2, Novosibirsk 630090, Russia, [3]International Tomography Center SB RAS, Institutskaya str. 3a, Novosibirsk 630090, Russia and [4]N. N. Vorozhtsov Novosibirsk Institute of Organic Chemistry SB RAS, pr. Lavrentjeva 9, Novosibirsk 630090, Russia

Received August 15, 2017; Revised October 23, 2017; Editorial Decision October 25, 2017; Accepted October 30, 2017

ABSTRACT

The model mRNA (MR), 11-mer RNA containing two nitroxide spin labels at the 5′- and 3′-terminal nucleotides and prone to form a stable homodimer $(MR)_2$, was used for Electron Paramagnetic Resonance study of structural rearrangements in mRNA occurring upon its binding to human 80S ribosomes. The formation of two different types of ribosomal complexes with MR was observed. First, there were stable complexes where MR was fixed in the ribosomal mRNA-binding channel by the codon-anticodon interaction(s) with cognate tRNA(s). Second, we for the first time detected complexes assembled without tRNA due to the binding of MR most likely to an exposed peptide of ribosomal protein uS3 away from the mRNA channel. The analysis of interspin distances allowed the conclusion that 80S ribosomes facilitate dissociation of the duplex $(MR)_2$: the equilibrium between the duplex and the single-stranded MR shifts to MR due to its efficient binding with ribosomes. Furthermore, we observed a significant influence of tRNA bound at the ribosomal exit (E) and/or aminoacyl (A) sites on the stability of ribosomal complexes. Our findings showed that a part of mRNA bound in the ribosome channel, which is not involved in codon-anticodon interactions, has more degrees of freedom than that interacting with tRNAs.

INTRODUCTION

RNAs are the key biopolymers of the cell due to their essential functions in the majority of the cell life events; in particular, they are involved in protein synthesis that is the final step of realization of the genetic information. These functions are generally associated with the interactions of RNAs with their molecular partners accompanied by changes in RNA structures, and monitoring of these changes for specific RNAs can provide important information for better understanding of the mechanisms of their functioning. Three kinds of RNA operate in the course of protein synthesis. First are ribosomal RNAs (rRNAs), constituents of ribosomes, large supramolecular ribonucleoprotein machineries that perform synthesis of polypeptides. Second are transfer RNAs (tRNAs) that carry amino acid residues to ribosomes for their subsequent incorporation into the nascent polypeptide chain. Third are messenger RNAs (mRNAs) carrying genetic information copied from DNA, which predetermines the amino acid sequences of the synthesized polypeptides in accordance with the universal genetic code, wherein each nucleotide triplet (codon) corresponds to one of amino acids or is a signal for stopping the translation. In the course of protein synthesis, mRNA is moving through the ribosome, where it interacts with tRNA molecules at three ribosomal sites named the A, P and E sites. The A (aminoacyl or acceptor) site is for incoming aminoacyl-tRNA cognate to mRNA codon bound at this site, the P (peptidyl or donor) site is for stable binding of tRNA bearing nascent peptide chain (peptidyl-tRNA), and the E (exit) site is for binding of the deacylated tRNA before it leaves the ribosome.

Many natural mRNAs have regions with rather stable local secondary structures. This can prevent their translation

*To whom correspondence should be addressed. Tel: +7 838 330 8850; Fax: +7 383 330 9752; Email: egbagryanskaya@nioch.nsc.ru
Correspondence may also be addressed to Matvey V. Fedin. Tel: +7 383 3301276; Fax: +7 383 3331399; Email: mfedin@tomo.nsc.ru
Correspondence may also be addressed to Galina G. Karpova. Tel: +7 383 3635140; Fax: +7 383 3635153; Email: karpova@niboch.nsc.ru

© The Author(s) 2017. Published by Oxford University Press on behalf of Nucleic Acids Research.
This is an Open Access article distributed under the terms of the Creative Commons Attribution License (http://creativecommons.org/licenses/by-nc/4.0/), which permits non-commercial re-use, distribution, and reproduction in any medium, provided the original work is properly cited. For commercial re-use, please contact journals.permissions@oup.com

by the ribosome, which is able to interact only with unstructured single-stranded (ss) mRNA sequences. Bacterial ribosomes can overcome this obstacle by their intrinsic helicase activity mediated by ribosomal proteins uS3, uS4 and uS5 located at the ribosomal mRNA entry site (1,2). In the eukaryotic translation system, the initiation factor eIF4A is involved in unfolding of the mRNA secondary structure in the course of translation (e.g. for review, see (3)). In higher eukaryotes, the translation of structured mRNAs also requires an additional protein, helicase DHX29 (4). For all that, the mRNA entry channel in the eukaryotic ribosome differs significantly from the analogous site of the bacterial ribosome (e.g. see (5,6)), and helicase activity of the eukaryotic ribosome itself has not yet been demonstrated. Electron paramagnetic resonance (EPR) spectroscopy is actively used in studies of structure, dynamics and conformational changes of nucleic acids and their complexes (7–23). Recently, using doubly spin-labeled short model ss-RNA, we have shown that the EPR nanometer-scale distance measurements can be successfully applied to study the state of mRNA in the human ribosome (24). Thus, we anticipate that the extension of this approach to model mRNA forming rather stable secondary structure would open up a nice possibility to monitor structural changes in such mRNA upon its binding to 80S ribosomes. In addition, the use of doubly spin-labeled model mRNA of suitable length can reveal the effect of A and/or E sites tRNAs on the stability of the complexes formed. Thus, the EPR distance measurements in complexes of 80S ribosomes with doubly spin-labeled model mRNA can yield information that has not yet been obtained using X-ray crystallography or cryo-electron microscopy.

In this study, a structured mRNA was modeled using a doubly spin-labeled 11-mer RNA (MR) with nitroxide groups at the C5 of the 5′-terminal uridine and at the C8 of the 3′-terminal adenosine. We found that this MR was able to form imperfect intermolecular duplexes, $(MR)_2$. The RNA sequence contained triplets coding for amino acids Val, Phe and Asp, any of which could be directed to the ribosomal P site by the interaction with the respective cognate tRNA targeted to this site. The binding of tRNAs cognate to MR triplets located at the A and/or E sites of 80S ribosomes associated with MR and P site tRNA resulted in the formation of complexes where the MR states resembled those of mRNA at certain steps of translation. In this way, various complexes of the MR with human ribosomes containing tRNA molecules either only at the P site or at the P and A, or at the P and E sites, or simultaneously at the P, A, and E sites, were prepared. Only deacylated tRNAs were used instead of peptidyl- and aminoacyl-tRNAs for the filling of P and A ribosomal sites, respectively. Nevertheless, in general, all the obtained complexes adequately reflected the states through which mRNA passes during translation in a real protein synthesis system. Monitoring of the interspin distances in these complexes allowed the estimation of the relative amount of the MR bound to the ribosome in each complex type. Moreover, for the first time we detected a binary complex of the vacant 80S ribosome with an mRNA analogue, which was not placed in the mRNA binding channel but was most likely associated with the region of the ribosomal protein (rp) uS3 exposed on the surface of the small (40S) ribosomal subunit away from this channel (25). We revealed differences between structures of MR bound to the ribosome in the mRNA binding channel and of MR bound most likely through an exposed rp uS3 fragment. We also found that tRNA bound at the A site and, especially, at the E site has a significant effect on the stability of the ribosomal complexes. In general, our findings shed light on previously unknown aspects of the interaction of mRNA with 80S ribosomes, thereby bringing novel insights into the molecular mechanisms of translation in eukaryotes.

MATERIALS AND METHODS

Preparation of doubly spin labeled RNA derivative

The spin label 3-carboxy-2,2,5,5-tetramethyl-2,5-dihydro-1H-pyrrol-1-oxyl succinimidyl ester (NHS-M2) was prepared according to the procedures described in Ref. (26) and used without deuteration, similar to our previous work (24). Undecaribonucleotide UGUGUUCGACA, whose 5′-terminal uridine and 3′-terminal adenosine bore ethylene diamine residues introduced at the C5 and C8 atoms, respectively, was synthesized and purified according to (27). The MR, doubly spin labeled RNA derivative that bore spin labels at the 5′ and 3′-terminal nucleotide bases, was prepared from the above oligomer by its treatment with NHS-M2 and subsequently purified as described in (24). Concentrations of the spin labels in sample containing MR were examined by EPR. Typically, the spin label concentrations calculated from the EPR data differed from those determined from the A_{260} absorption of the doubly spin-labeled RNA by no more than 40%. In the latter case, we assumed that one A_{260} unit of the 11-mer corresponds to 8600 pmol (which was calculated taking into account the molar extinction coefficient of the 11-mer and neglecting the coefficient of the spin label that was very low).

Ribosomes and tRNAs

40S and 60S ribosomal subunits were isolated from unfrozen human placenta as described in (28). At the final step of preparation, the 60S and 40S subunits were re-suspended in D_2O up to concentrations of 35 pmol/μl and 45 pmol/μl, respectively, and stored in liquid nitrogen in small aliquots, each of which was unfrozen only once. Prior to use, the subunits were re-activated by incubation in binding buffer A (50 mM Tris–HCl, pH 7.5, 100 mM KCl, 13 mM $MgCl_2$ and 0.5 mM EDTA in D_2O) at 37°C for 10 min; 80S ribosomes were obtained by association of re-activated 40S and 60S subunits taken in a 40S:60S ratio of 1:1.3. The activity of the ribosomes in the poly (U)-directed binding of [^{14}C]Phe–tRNA^{Phe} was about 80%. tRNA^{Phe} and tRNA^{Val} (both about 1300 pmol/A260 unit) from *Escherichia coli* were the kind gifts from Dr V.I. Katunin (National Research Center 'Kurchatov Institute' B.P. Konstantinov St. Petersburg Nuclear Physics Institute). Yeast tRNA^{Asp} transcript obtained by *in vitro* T7 transcription was used as tRNA^{Asp}. Prior to use for binding to the ribosomes, tRNAs were re-activated by incubation in buffer A at 37°C for 5 min.

Analysis of functional competence of MR as mRNA analogue

MR or tRNAs were labelled at their 5′-termini by gamma-^{32}P-ATP and polynucleotide kinase as described (24). Mixtures for experiments on the analysis of binding of labeled MR to 80S ribosomes contained in 7 μl of buffer A 5.2 pmol of 80S ribosomes, 25 pmol of tRNA^{Phe} and 4–45 pmol of labeled MR; in parallel, experiments without tRNA^{Phe} were carried out. After incubation at 20°C for 1 h, the mixtures were filtered through nitrocellulose filters (pore diameter 0.45 μM), which bind ribosomes but not low molecular mass RNAs, as described before (29). The amount of radioactivity bound to filters was measured by Cherenkov counting, and the amount of bound MR in pmol was calculated from the known specific radioactivity of the labeled RNA. The MR binding levels were corrected for background sorption of the labeled RNA on filters by subtracting of the values obtained in parallel by filtration of the mixtures containing the respective amounts of labeled MR without ribosomes and tRNA. Binding of labeled tRNA^{Val} or tRNA^{Phe} to the E site of 80S ribosomes in the presence of MR as an mRNA analogue was examined similarly. At first, ternary complex of the ribosomes (7.5 pmol) with MR (70 pmol) and unlabeled tRNA^{Phe} (10 pmol) targeted to the P site was formed by incubation of the components in buffer A for 1 h, then 10–60 pmol of labeled tRNA was added (final volume of the reaction mixtures was 7.5 μl) with subsequent incubation for 2 h.

Ribosomal complexes for the EPR experiments

The binary complex was obtained by the incubation of MR (13.5 μM) and ribosomes (15 μM) for 1 h. To obtain the ternary ribosomal complex containing MR as an mRNA analogue and tRNA^{Phe} at the P site, 180 pmol of 40S subunits were first incubated with 162 pmol of tRNA^{Phe} in 4.85 μl of buffer A for 20 min. After this, 162 pmol of MR in 0.55 μl of buffer A was added and the mixture was incubated for 1 h with subsequent addition of 200 pmol of 60S subunits in 6.25 μl of buffer A and incubation for 2 h. To prepare ribosomal complex with codon-anticodon interactions at both A and P sites, the ternary complex obtained as described above was mixed with 234 pmol of tRNA^{Asp} with subsequent incubation for 1 h. The binding of tRNA^{Val} or tRNA^{Phe} at the E site of the ribosomal ternary complex or the complex with tRNAs at both the A and P sites was carried out by incubation of these complexes with 0.5 μl of buffer A containing 324 pmol of tRNA^{Val} or tRNA^{Phe} for 1 h. Before EPR analysis, samples that did not contain ribosomes were supplied with glycerol-d_8 (0.7 μl of glycerol-d_8 per each μl of the sample mixture).

EPR experiments

Samples for Double Electron-Electron Resonance (DEER/PELDOR) measurements were prepared at room temperature in glass capillary tubes (OD 1.5 mm, ID 0.9 mm, with the sample volume being ca. 10 μl), shock-frozen in liquid nitrogen and investigated at $T = 50$ K. The data were collected at the Q-band (34 GHz) using a Bruker Elexsys E580 pulse EPR spectrometer equipped with an EN5107D2 resonator and Oxford Instruments temperature control system (maximum available microwave power was limited to 1 W). A standard four-pulse DEER sequence (30) was used with pulse lengths of 22/44 ns for probe (υ_{probe}) and 44 ns for pump (υ_{pump}) frequency and with two-step phase cycle. The time increment of the inversion pulse was 6 ns. The values of τ_1 and τ_2 (Supplementary Figure S1 in SI) were 400 ns and 3500 ns, correspondingly. The measurements were done at a field position of ~2.5 mT higher than the maximum of the spectrum, thus using $\Delta\upsilon = (\upsilon_{pump} - \upsilon_{probe}) = 70$ MHz led to the pump pulse applied at the spectral maximum. All obtained DEER traces were background corrected by exponential function and analyzed with Tikhonov regularization using DeerAnalysis2013 program (31).

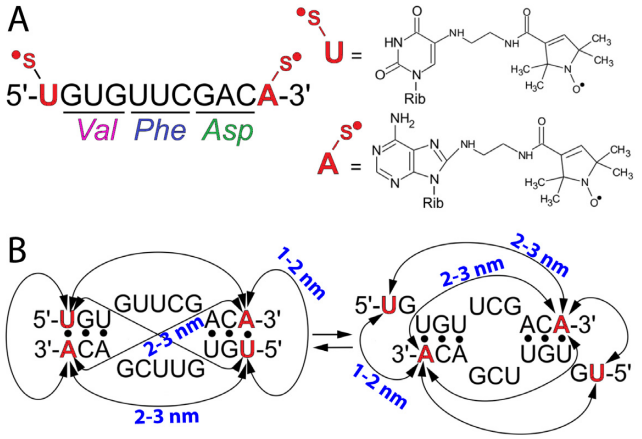

Figure 1. Model doubly spin-labeled RNA (MR) used in this study and its intermolecular duplexes. (**A**) the sequence of MR, in which triplets coding for Val, Phe and Asp are underlined; on the right, structures of the terminal MR nucleotides bearing spin labels are presented. (**B**) possible structures of intermolecular duplexes $(MR)_2$ and calculated interspin distances in the ss-MR and in its duplexes.

RESULTS AND DISCUSSION

Model RNA and its complexes

The MR used in this study (Figure 1) contained sequential triplets GUG, UUC and GAC coding for Val, Phe and Asp, respectively, and nitroxide spin labels introduced via ethylene diamine linker at the 5′-terminal uridine and at the 3′-terminal adenosine. This MR has several differences from the doubly spin-labeled RNA that we have previously utilized to explore the state of mRNA in the human ribosome (24). First, the label attachment sites in RNA are different; in particular, the linker for the attachment of the 5′-terminal label is at the C5 of the 5′-terminal uridine in MR, but not at the 5′-terminal phosphate as in our previous work. Second, the label at C8 of the 3′-terminal adenosine is separated from the label at the 5′-terminal nucleotide residue by nine residues (versus four ones previously). Moreover, MR is potentially able to form two kinds of imperfect bimolecular duplexes $(MR)_2$ (Figure 1), in which the interspin distance is expected to be much smaller than that in the ss-RNA.

The design of ribosomal complexes in this study was based on the well-known fact that in the absence of translation factors at elevated Mg^{2+} concentrations tRNA has

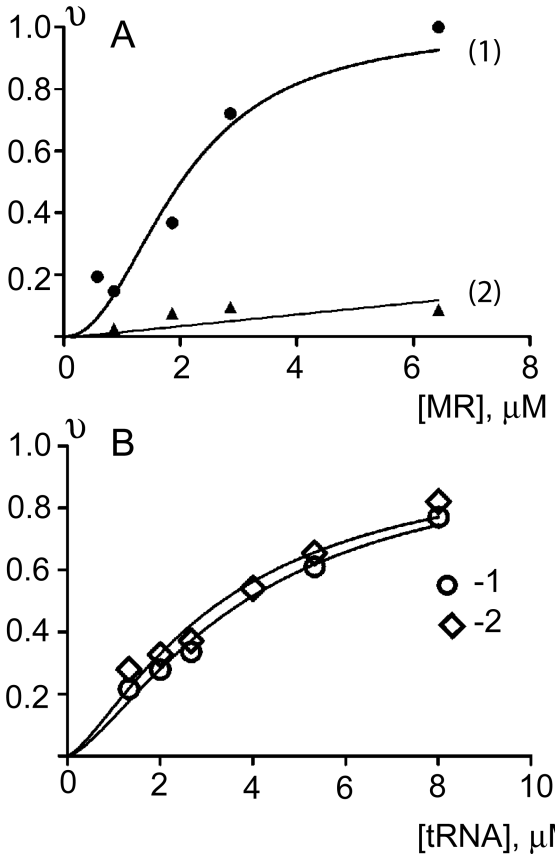

Figure 2. Examination of the binding of MR and E site tRNA to 80S ribosomes. (**A**), isotherms of binding of 5′-^{32}P-labeled MR to 80S ribosomes in the presence of tRNA^{Phe} (1) and without tRNA (2); υ, MR binding level (mol of mRNA analogue per mol of 80S ribosomes) normalized to the fraction of active ribosomes. (**B**), isotherms of binding of 5′-^{32}P-labeled tRNA^{Val} (1) and tRNA^{Phe} (2) to the complex of 80S ribosomes with MR and tRNA^{Phe} at the P site; υ, binding level of the labeled tRNA (mol of labeled tRNA per mol of 80S ribosomes) normalized to the fraction of active ribosomes.

considerable preferential affinity to the P site (for a review, see (32)), where it can interact with a cognate mRNA codon, thereby fixing mRNA on the ribosome. Besides, it is worth noting that the short ss-RNA practically does not bind at the ribosomal mRNA-binding channel in the absence of an appropriate tRNA. The results presented in Figure 2A show that 80S ribosomes can be completely saturated with the MR. The formation of a stable complex of MR with ribosomes is almost completely dependent on the presence of tRNA^{Phe}, demonstrating that MR is a functionally competent mRNA analogue. The K_d value of 2.0 ± 0.6 μM calculated from the binding data implies that at the concentrations of MR and 80S ribosomes used for EPR the major fraction of the components should exist as a complex. This value is about 2.5-fold smaller than that reported for the doubly spin-labeled 9-mer RNA utilized previously (24). Obviously, this occurs because 80S ribosomes used here bind mRNA tighter than the isolated 40S subunits examined in (24).

When the mRNA analogue is tightly fixed on the ribosome by the codon-anticodon interaction with cognate

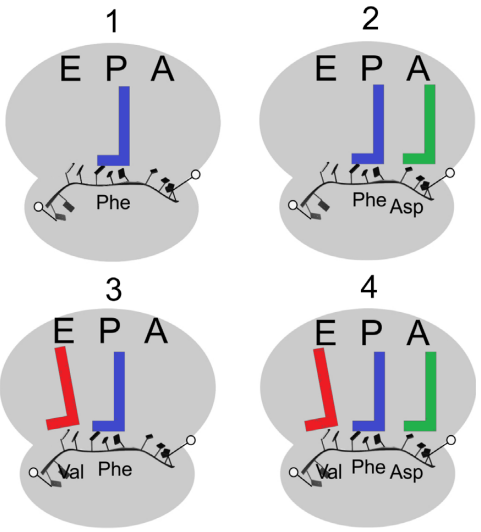

Figure 3. Schemes of complexes formed based on 80S ribosomes associated with MR fixed in the mRNA channel by the codon-anticodon interaction with tRNA^{Phe} at the P site. tRNAs bound at the P, A and E sites are shown as L-shaped images.

tRNA at the P site (Figure 3, complex 1), the designed triplets occur at the A and the E sites, and the respective cognate tRNAs can be bound at these sites leading to the formation of complexes 2–4 (Figure 3). The binding of a non-cognate tRNA at the E site is possible as well, and the obligatory occurrence of the codon-anticodon interaction at this site still remains in question. The occupation of the ribosomal A site with tRNA under conditions very similar to those used here has been demonstrated in our previous study with a doubly spin-labeled mRNA analogue, where a triplet targeted to the A site contained a spin label at the C8 of adenosine residue in third position (24). Since in this study the label was attached in the same way to nucleotide adjacent to the triplet directed to the A site, binding of tRNA at this site should occur. With respect to MR, we showed that spin label at the nucleotide adjacent to the triplet directed to the E site does not prevent the binding of cognate and non-cognate tRNA at the E site and both kinds of tRNAs have similar affinity to this ribosomal site (Figure 2B).

Complexes 1–4 (Figure 3) applied in this study mimic functional states of the ribosome occurring in the course of polypeptide synthesis. In particular, complex 1 resembles that formed at the final step of initiation of peptide synthesis; it corresponds to the state of ribosome ready to accept the first aminoacyl-tRNA at the A site at the first elongation cycle (in the protein-synthesizing ribosome, the P site at this step is occupied with initiator Met-tRNAi). Complexes 2–4 mimic various states of the ribosome taking place in the course of elongation of polypeptide chain. In particular, complex 2 resembles the pre-translocation state, which takes place after accommodation of the upcoming cognate aminoacyl-tRNA at the A site. Complex 3 mimics the post-translocation state after peptide transfer and translocation of the elongated peptidyl-tRNA from the A to the P site and discarded deacylated tRNA from the P to the E site.

Complex 4 represents a state that could occur upon binding of upcoming aminoacyl-tRNA at the A site of the complex where the E site tRNA did not yet leave the ribosome. One has to note that our model complexes are simplified, namely, tRNAs bound at the P and A sites do not contain peptidyl or aminoacyl residues at their 3′-termini. However, deacylated tRNAs are applicable here because we examine the structure of ribosome-bound mRNA, and our earlier studies on cross-linking of chemically reactive mRNA analogues to human ribosomes (33–36) have shown that the arrangement of mRNA relative to the ribosomal components does not depend on the presence of an aminoacyl- or peptidyl moiety at the 3′-end of tRNA interacting with the mRNA codons.

At present, it is already known that unstructured RNAs can bind to 80S ribosomes not only in the mRNA channel but also at alternative sites. In particular, recently it has been shown that various chemically reactive derivatives of short ss-RNAs are able to form a specific cross-link to peptide 54–62 in so-called KH domain of rp uS3 exposed on the surface of the 40S subunit of the human ribosome. This peptide is located away from the mRNA binding channel, and its cross-linking to ss-RNAs does not depend on the presence of tRNA (25). Structures of labile ribosomal complexes where ss-RNA is bound to ribosomes via this exposed uS3 fragment are unknown in contrast to the structures of stable complexes of eukaryotic ribosomes with mRNAs and tRNAs, which have been visualized by cryo-electron microscopy (e.g. see (37–39)) and by X-ray crystallography (40). Moreover, the above-mentioned labile complexes have not even been directly detected yet. This is probably due to the insufficiently high concentrations of ribosomes and ss-RNAs used in the studies, although the indication of the formation of such complexes was obtained in our previous work (24). In this study, we applied concentrations of 80S ribosomes and MR more than one order of magnitude higher than those typically used before. Therefore, we reasonably expected to detect the above-mentioned type binary complex and to obtain information on alterations of the RNA structure accompanying this complex formation.

Monitoring of rearrangements of the MR structure caused by its binding to ribosomes

To measure the interspin distances between two nitroxide labels of MR, we employ here DEER, (also known as PELDOR) in 4-pulse version (30). Figure 4 shows the obtained DEER time traces and distance distributions for MR and its complexes. The obtained mean distances $<r_{DEER}>$ and corresponding standard deviation parameters σ are summarized in Table 1. For isolated MR the distance distribution consists mainly of one peak with average distance $<r_{DEER}> = 2.5$ nm, that is significantly shorter than the expected distance 4.1 nm between nucleotide's atoms bearing spin labels in the ss-RNA. However, this measured distance is in good agreement with the expected separation of 2–3 nm between the terminal nucleotides in the duplex formed by two molecules of MR and being in the A form helix (Figure 1B). The formation of dimers is also indicated by additional line broadening (0.5 mT) observed in the continuous wave (CW) EPR spectrum at 300 K. Such broadening is reasonably ascribed to dipolar interaction between spin labels located on one side of the duplex and separated by ∼1–2 nm (see Supporting Information (SI)). In addition, the modulation depth in DEER time traces agrees well with the formation of dimer (see SI for more details).

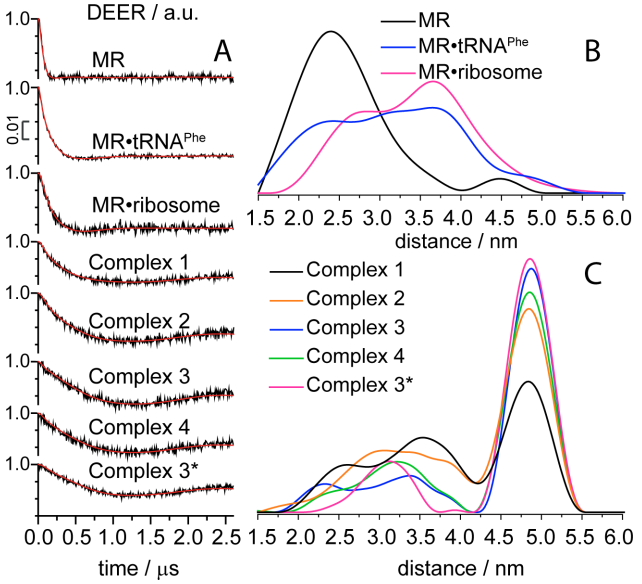

Figure 4. Distance measurements in isolated MR, in the binary mixtures with tRNA or 80S ribosomes and in the ribosomal complexes with tRNA(s) obtained by Q-band DEER. Complex 3* corresponds to complex 3 with non-cognate E site tRNA. (**A**) Background corrected four-pulse DEER traces (intensity is normalized). Lines with noise correspond to the experimental data. Solid lines show best fits obtained using DeerAnalysis2013. (**B** and **C**) Obtained distance distribution for the mixtures and complexes after normalization. Regularization parameter *L* is 1000.

In the presence of free 80S ribosomes, distance measurements clearly display two MR fractions (Figure 4, MR•ribosome). The $<r_{DEER}>$ value of the smaller one is close to that for the isolated MR, whereas $<r_{DEER}>$ of the larger one is ∼3.6 nm, which certainly corresponds to the binary complex of ribosomes with MR (Table 1). The results obtained with all ribosomal complexes 1–4 containing $tRNA^{Phe}$ show the appearance of the major peak at $<r_{DEER}>$ ∼4.9 nm. This peak can only be assigned to the mRNA fixed at the ribosomal binding site by the codon-anticodon interaction with tRNA(s), because in the reference experiment with binary mixture of $tRNA^{Phe}$ with MR (without ribosomes) this peak is absent (Figure 4). The binding of MR to ribosome was also confirmed by room-temperature CW EPR measurements revealing the onset of additional fraction of spin labels with the slow anisotropic motion (SI). Finally, the suppression of electron-nuclear interactions between nitroxides and D_2O molecules in the complex compared to isolated MR is also supportive of the above explanation (see SI for ESEEM study).

In order to estimate the weights of different MR conformations, the integrals over obtained distance distributions were normalized. Quantification of the results given in Table 1 demonstrates that ∼45% of MR is bound at the mRNA channel in the ribosomal complex with P site $tRNA^{Phe}$ (complex 1), which is in a satisfactory agreement

Table 1. Mean distances $<r_{DEER}>$ and standard deviation parameters σ obtained by EPR for all studied complexes. For uniform processing of the results, three distance ranges were selected where representative peaks are located. For a peak with $<r_{DEER}> \sim 4.9$ nm that corresponds to MR fixed at mRNA binding channel, its weight relative to the total signal is shown in parentheses

Complex type	$<r_{DEER}> \pm \sigma$ (nm)		
	Range 1.5–4.0 nm		Range 4.0–6.0 nm
	1.5–3.0 nm	3.0–4.2 nm	
MR	2.51 ± 0.5		
MR/tRNA^{phe}	2.4 ± 0.4	3.6 ± 0.3	
MR/80S	2.6 ± 0.3	3.6 ± 0.3	
Complex 1	2.6 ± 0.3	3.6 ± 0.3	4.8 ± 0.3 (0.46)
Complex 2	2.6 ± 0.3	3.5 ± 0.3	4.8 ± 0.3 (0.59)
Complex 3	2.5 ± 0.3	3.4 ± 0.3	4.9 ± 0.2 (0.74)
Complex 4	2.6 ± 0.3	3.4 ± 0.3	4.9 ± 0.2 (0.71)
Complex 3* (with non-cognate E site tRNA)	3.1±0.3		4.9 ± 0.2 (0.81)

with the K_d value corresponding to this type of binding (see the previous section). Note that K_d value can, in principle, change to some extent upon low-temperature PELDOR measurements compared to room temperature; however, implementation of shock-freezing minimizes this possibility.

In addition, one can see two minor peaks corresponding to the binary complex of ribosomes with MR ($<r_{DEER}> \sim$ 3.6 nm, see above) and to the isolated ss-RNA ($<r_{DEER}> \sim$ 2.6 nm).

Evidently, the addition of tRNAs directed to the A and/or the E sites increases the fraction of MR bound at the mRNA channel (Figure 4, Table 1). This trend agrees with the expectations, because the fixation of mRNA on the ribosome by two or three codon-anticodon interactions should be stronger compared to single interaction at the P site, and therefore an equilibrium between the duplex $(MR)_2$ and the MR bound to the ribosome shifts to the latter. Interestingly, tRNA directed to the E site (complex 3) increases the amount of MR bound at the mRNA channel to a higher extent compared to the case where tRNA is directed to the A site (complex 2) (Figure 4, Table 1). This observation agrees well with previous data on higher affinity of deacylated tRNA to the E site than to the A site of bacterial ribosomes (41). What seems somewhat unexpected is that the effect of a non-cognate tRNA directed to the E site is almost the same as that of the cognate tRNA (Figure 4, Table 1). These results indicate that the effect of the E site binding of tRNA on the strength of mRNA fixation in the ribosome is caused by a reason other than the codon-anticodon interaction. The latter argues against realization of codon-anticodon interactions at the E site that had been postulated earlier (e.g. see (42)). One can assume that the stabilizing effect is indirect, e.g. tRNA molecule bound at the E site changes ribosomal structure of this site in the region of the mRNA binding channel, making it more favorable for mRNA fixation therein.

Binding of ss-RNA to the 40S subunit away from the mRNA binding channel

The use of very high concentrations of ribosomes and MR actually allowed us to detect the structure adopted by RNA when it binds to vacant 80S ribosomes. In the respective binary mixture, more than $\frac{1}{2}$ of the total amount of MR changed its structure to that with $<r_{DEER}> \sim 3.6$ nm. This value is significantly larger than that of the MR duplex but considerably less than $<r_{DEER}>$ of the ss-RNA and the RNA bound at the mRNA channel (4.9 nm, see above). The results obtained clearly indicate that the structure of MR bound to vacant 80S ribosomes significantly differs from the structure of both $(MR)_2$ and of MR fixed at the ribosomal mRNA channel by the codon-anticodon interaction with tRNA(s) (Figure 4). In addition, the formation of a specific complex of MR with 80S ribosome even in the absence of tRNA was also supported by ESEEM studies and measurements of phase relaxation time (T_m) (see SI).

As mentioned above, binding of short ss-RNAs to vacant 80S ribosomes is most likely mediated by an exposed fragment of rp uS3 away from the mRNA channel (25). Our results for the first time shed light on the structure of RNA bound to the ribosome in this way. The smaller $<r_{DEER}>$ value for the binary complex than that for the free ss-MR or for the RNA bound at the mRNA channel (Figure 4) points out to the more curved MR structure in this complex. It is noteworthy that similar values of $<r_{DEER}>$ for the binary complexes MR•ribosome and MR•tRNA^{Phe} may reflect some degree of similarity of the structures of binary complexes of these types. Obviously, the latter complex is formed due to the interaction of triplet UUC of the MR with the complementary anticodon of tRNA^{Phe} (43). By analogy, one can assume that the RNA stretch interacting with the ribosome-bound rp uS3 is also as short as the length of ca. three nucleotides, which is consistent with labile nature of binary complexes of ss-RNAs with ribosomes mediated by an exposed rp uS3 fragment.

How structured RNA binds to 80S ribosomes?

Our results indicate that under conditions in which >95% of an isolated RNA exists as a duplex, 80S ribosomes can effectively form two principally different kinds of complexes containing the respective RNA in the single-stranded form; the higher the stability of ribosomal complexes formed, the larger the portion of MR unfolded and bound to ribosomes. In particular, the yield of the labile complex MR•ribosome, where RNA binding is mediated by an exposed uS3 fragment ($<r_{DEER}> \sim 3.6$ nm), is maximum in the absence of tRNA when the RNA is unable to bind at the ribosomal mRNA channel. Accordingly, in this case the share of non-

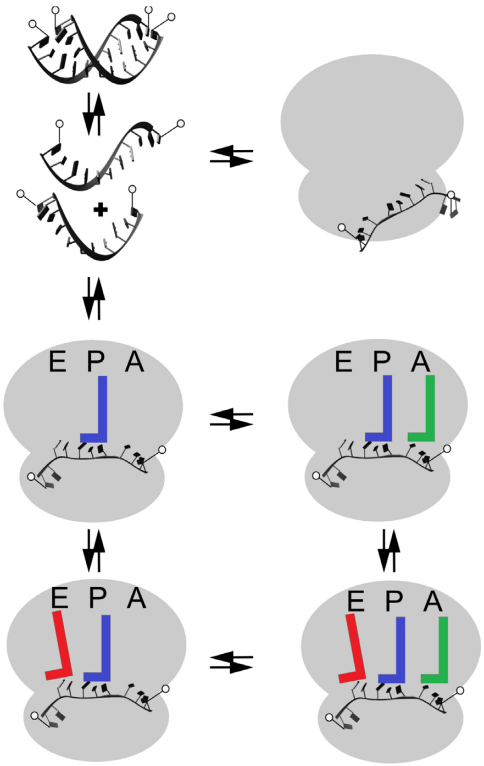

Figure 5. The suggested scheme of equilibria between different states of MR: free, organized in a duplex and bound to 80S ribosomes in different ways.

dissociated $(MR)_2$ is larger than in all other mixtures, which is in agreement with the least stable nature of the ribosomal complex formed. When the binding occurs in the presence of the P site $tRNA^{Phe}$, the yield of MR bound to the ribosome via uS3 ($<r_{DEER}> \sim 3.6$ nm) and the share of non-dissociated $(MR)_2$ significantly decrease, and the major fraction of MR appears in the mRNA binding channel ($<r_{DEER}> \sim 4.9$ nm). In the complexes where MR is additionally stabilized at the mRNA channel by two or three tRNAs, the shares of the non-dissociated $(MR)_2$ and MR bound to ribosome via uS3 become even smaller as compared to the major fraction of MR bound at the channel. All this implies that dissociation of the duplex $(MR)_2$ and the subsequent binding of the ss-MR to ribosomes occurs without action of ribosomal helicase. The binding can be simply described by equilibria between MR and $(MR)_2$, between the MR free and bound to ribosomes via uS3, and also between the MR free and bound at the ribosomal mRNA channel (Figure 5). The more stable the complex, the stronger the equilibrium is shifted towards its formation.

CONCLUSION

The application of a model RNA capable of forming a rather stable duplex and bearing two spin labels at the 5′-terminal and 3′-terminal nucleotide bases enabled us to monitor the disruption of the RNA duplex and the subsequent formation of various types of complexes of the ss-RNA with human 80S ribosomes using EPR spectroscopy. We showed that the unfolding of RNA preceding its binding to the ribosome is the result of a shift in the equilibrium between RNA in single-stranded and double-stranded forms, and between ss-RNA free and bound to ribosomes through an exposed uS3 fragment or in the mRNA channel. This implies that ribosomal helicase activity does not promote the RNA unfolding. We also revealed that the A site- and E site-bound tRNA contribute to the stability of the ribosomal complexes, in which mRNA is placed in the mRNA binding channel by tRNA targeted at the P site. It turned out that the greater contribution is made by E site tRNA, no matter if it is cognate or non-cognate to the codon in this site. Thus, the approach used allowed us to distinguish the structures of RNA bound to 80S ribosomes in complexes of different nature, thereby providing means for the first direct detection of the labile binary complex of ss-RNA with the 80S ribosome, the formation of which is most likely mediated by an exposed peptide of the KH domain of rp uS3. In addition, we found that the E site tRNA tightens the mRNA binding to the ribosome and that this effect does not depend on whether tRNA is cognate to the E site mRNA codon. This clearly shows that the E site tRNA maintains the mRNA path through the ribosome without the implication of codon-anticodon interactions, thereby contributing to an understanding of the role of the E site tRNA in the mechanism of protein synthesis.

SUPPLEMENTARY DATA

Supplementary Data are available at NAR online.

FUNDING

Russian Science Foundation [14-14-00922]. Funding for open access charge: Russian Science Foundation [14-14-00922].
Conflict of interest statement. None declared.

REFERENCES

1. Borovinskaya,M.A., Shoji,S., Holton,J.M., Fredrick,K. and Cate,J.H.D. (2007) A steric block in translation caused by the antibiotic spectinomycin. *ACS Chem. Biol.*, **2**, 545–552.
2. Takyar,S., Hickerson,R.P. and Noller,H.F. (2005) mRNA helicase activity of the ribosome. *Cell*, **120**, 49–58.
3. Hinnebusch,A.G. (2014) The scanning mechanism of eukaryotic translation initiation. *Annu. Rev. Biochem.*, **83**, 779–812.
4. Pisareva,V.P., Pisarev,A.V., Komar,A.A., Hellen,C.U.T. and Pestova,T.V. (2008) Translation initiation on mammalian mRNAs with structured 5'UTRs requires DExH-box protein DHX29. *Cell*, **135**, 1237–1250.
5. Rabl,J., Leibundgut,M., Ataide,S.F., Haag,A. and Ban,N. (2011) Crystal structure of the eukaryotic 40S ribosomal subunit in complex with initiation factor 1. *Science*, **331**, 730–736.
6. Ben-Shem,A., Garreau de Loubresse,N., Melnikov,S., Jenner,L., Yusupova,G. and Yusupov,M. (2011) The structure of the eukaryotic ribosome at 3.0 Å resolution. *Science*, **334**, 1524–1529.
7. Duss,O., Michel,E., Yulikov,M., Schubert,M., Jeschke,G. and Allain,F.H.-T. (2014) Structural basis of the non-coding RNA RsmZ acting as a protein sponge. *Nature*, **509**, 588–592.
8. Duss,O., Yulikov,M., Jeschke,G. and Allain,F.H.-T. (2014) EPR-aided approach for solution structure determination of large RNAs or protein-RNA complexes. *Nat. Commun.*, **5**, 3669.
9. Babaylova,E.S., Malygin,A.A., Lomzov,A.A., Pyshnyi,D.V., Yulikov,M., Jeschke,G., Krumkacheva,O.A., Fedin,M.V., Karpova,G.G. and Bagryanskaya,E.G. (2016)

Complementary-addressed site-directed spin labeling of long natural RNAs. *Nucleic. Acids. Res.*, **44**, 7935–7943.
10. Piton,N., Mu,Y., Stock,G., Prisner,T.F., Schiemann,O. and Engels,J.W. (2007) Base-specific spin-labeling of RNA for structure determination. *Nucleic. Acids. Res.*, **35**, 3128–3143.
11. Grant,G.P.G. and Qin,P.Z. (2007) A facile method for attaching nitroxide spin labels at the 5′ terminus of nucleic acids. *Nucleic. Acids. Res.*, **35**, e77.
12. Cai,Q., Kusnetzow,A.K., Hubbell,W.L., Haworth,I.S., Gacho,G.P.C., Van Eps,N., Hideg,K., Chambers,E.J. and Qin,P.Z. (2006) Site-directed spin labeling measurements of nanometer distances in nucleic acids using a sequence-independent nitroxide probe. *Nucleic. Acids. Res.*, **34**, 4722–4730.
13. Schiemann,O., Piton,N., Mu,Y., Stock,G., Engels,J.W. and Prisner,T.F. (2004) A PELDOR-Based Nanometer Distance Ruler for Oligonucleotides. *J. Am. Chem. Soc.*, **126**, 5722–5729.
14. Shevelev,G.Y., Krumkacheva,O.A., Lomzov,A.A., Kuzhelev,A.A., Rogozhnikova,O.Y., Trukhin,D.V., Troitskaya,T.I., Tormyshev,V.M., Fedin,M.V., Pyshnyi,D.V. *et al.* (2014) Physiological-temperature distance measurement in nucleic acid using triarylmethyl-based spin labels and pulsed dipolar EPR spectroscopy. *J. Am. Chem. Soc.*, **136**, 9874–9877.
15. Grohmann,D., Klose,D., Klare,J.P., Kay,C.W.M., Steinhoff,H.J. and Werner,F. (2010) RNA-binding to archaeal RNA polymerase subunits F/E: A DEER and FRET study. *J. Am. Chem. Soc.*, **132**, 5954–5955.
16. Schiemann,O., Weber,A., Edwards,T.E., Prisner,T.F. and Sigurdsson,S.T. (2003) Nanometer distance measurements on RNA using PELDOR. *J. Am. Chem. Soc.*, **125**, 3434–3435.
17. Sowa,G.Z. and Qin,P.Z. (2008) Site-directed spin labeling studies on nucleic acid structure and dynamics. *Prog. Nucleic Acid Res. Mol. Biol.*, **82**, 147–197.
18. Bagryanskaya,E.G., Krumkacheva,O.A., Fedin,M.V. and Marque,S.R.A. (2015) Development and application of spin traps, spin probes, and spin labels. *Methods Enzymol.*, **563**, 365–396.
19. Shevelev,G.Y., Krumkacheva,O.A., Lomzov,A.A., Kuzhelev,A.A., Trukhin,D.V., Rogozhnikova,O.Y., Tormyshev,V.M., Pyshnyi,D.V., Fedin,M.V. and Bagryanskaya,E.G. (2015) Triarylmethyl labels: toward improving the accuracy of EPR nanoscale distance measurements in DNAs. *J. Phys. Chem. B*, **119**, 13641–13648.
20. Babaylova,E.S., Ivanov,A.V., Malygin,A.A., Vorobjeva,M.A., Venyaminova,A.G., Polienko,Y.F., Kirilyuk,I.A., Krumkacheva,O.A., Fedin,M.V., Karpova,G.G. *et al.* (2014) A versatile approach for site-directed spin labeling and structural EPR studies of RNAs. *Org. Biomol. Chem.*, **12**, 3129–3136.
21. Kim,N.K., Bowman,M.K. and Derose,V.J. (2010) Precise mapping of RNA tertiary structure via nanometer distance measurements with double electron-electron resonance spectroscopy. *J. Am. Chem. Soc.*, **132**, 8882–8884.
22. Zhang,X., Tung,C.S., Sowa,G.Z., Hatmal,M.M., Haworth,I.S. and Qin,P.Z. (2012) Global structure of a three-way junction in a Phi29 packaging RNA dimer determined using site-directed spin labeling. *J. Am. Chem. Soc.*, **134**, 2644–2652.
23. Sicoli,G., Wachowius,F., Bennati,M. and Höbartner,C. (2010) Probing secondary structures of spin-labeled RNA by pulsed EPR spectroscopy. *Angew. Chemie Int. Ed.*, **49**, 6443–6447.
24. Malygin,A.A., Graifer,D.M., Meschaninova,M.I., Venyaminova,A.G., Krumkacheva,O.A., Fedin,M.V., Karpova,G.G. and Bagryanskaya,E.G. (2015) Doubly spin-labeled RNA as an EPR reporter for studying multicomponent supramolecular assemblies. *Biophys. J.*, **109**, 2637–2643.
25. Sharifulin,D.E., Grosheva,A.S., Bartuli,Y.S., Malygin,A.A., Meschaninova,M.I., Ven'yaminova,A.G., Stahl,J., Graifer,D.M. and Karpova,G.G. (2015) Molecular contacts of ribose-phosphate backbone of mRNA with human ribosome. *Biochim. Biophys. Acta*, **1849**, 930–939.
26. Hankovszky,H.O., Hideg,K. and Tigyi,J. (1978) Nitroxides. Ii. 1-oxyl-2,2,5,5-tetramethylpyrroline-3-carboxylic acid derivatives. *Acta Chir. Acad. Sci. Hung.*, **98**, 339–348.
27. Repkova,M.N., Ivanova,T.M., Komarova,N.I., Meshchaninova,M.I., Kuznetsova,M.A. and Venyaminova,A.G. (1999) H-phosphonate synthesis of oligoribonucleotides containing modified bases. I. Photoactivatable derivatives of oligoribonucleotides with perfluoroarylazide groups in heterocyclic bases. *Russ. J. Bioorgan. Chem.*, **25**, 690–701.
28. Matasova,N.B., Myltseva,S.V., Zenkova,M.A., Graifer,D.M., Vladimirov,S.N. and Karpova,G.G. (1991) Isolation of ribosomal subunits containing intact rRNA from human placenta: estimation of functional activity of 80S ribosomes. *Anal. Biochem.*, **198**, 219–223.
29. Graifer,D.M., Malygin,A.A., Matasova,N.B., Mundus,D.A., Zenkova,M.A. and Karpova,G.G. (1997) Studying functional significance of the sequence 980–1061 in the central domain of human 18S rRNA using complementary DNA probes. *Biochim. Biophys. Acta*, **1350**, 335–344.
30. Pannier,M., Veit,S., Godt,A., Jeschke,G. and Spiess,H. (2000) Dead-time free measurement of dipole–dipole interactions between electron spins. *J. Magn. Reson.*, **142**, 331–340.
31. Jeschke,G., Chechik,V., Ionita,P., Godt,A., Zimmermann,H., Banham,J., Timmel,C.R., Hilger,D. and Jung,H. (2006) DeerAnalysis2006—a comprehensive software package for analyzing pulsed ELDOR data. *Appl. Magn. Reson.*, **30**, 473–498.
32. Graifer,D. and Karpova,G. (2013) Photoactivatable RNA derivatives as tools for studying the structural and functional organization of complex cellular ribonucleoprotein machineries. *RSC Adv.*, **3**, 2858–2872.
33. Bulygin,K.N., Graifer,D.M., Repkova,M.N., Smolenskaya,I.A., Veniyaminova,A.G. and Karpova,G.G. (1997) Nucleotide G-1207 of 18S rRNA is an essential component of the human 80S ribosomal decoding center. *RNA*, **3**, 1480–1485.
34. Demeshkina,N., Repkova,M., Ven'yaminova,A., Graifer,D. and Karpova,G. (2000) Nucleotides of 18S rRNA surrounding mRNA codons at the human ribosomal A, P, and E sites: a crosslinking study with mRNA analogs carrying an aryl azide group at either the uracil or the guanine residue. *RNA*, **6**, 1727–1736.
35. Demeshkina,N., Laletina,E., Meschaninova,M., Ven'yaminova,A., Graifer,D. and Karpova,G. (2003) Positioning of mRNA codons with respect to 18S rRNA at the P and E sites of human ribosome. *Biochim. Biophys. Acta*, **1627**, 39–46.
36. Graifer,D., Molotkov,M., Styazhkina,V., Demeshkina,N., Bulygin,K., Eremina,A., Ivanov,A., Laletina,E., Ven'yaminova,A. and Karpova,G. (2004) Variable and conserved elements of human ribosomes surrounding the mRNA at the decoding and upstream sites. *Nucleic. Acids. Res.*, **32**, 3282–3293.
37. Brown,A., Shao,S., Murray,J., Hegde,R.S. and Ramakrishnan,V. (2015) Structural basis for stop codon recognition in eukaryotes. *Nature*, **524**, 493–496.
38. Budkevich,T.V., Giesebrecht,J., Behrmann,E., Loerke,J., Ramrath,D.J.F., Mielke,T., Ismer,J., Hildebrand,P.W., Tung,C.-S., Nierhaus,K.H. *et al.* (2014) Regulation of the mammalian elongation cycle by subunit rolling: a eukaryotic-specific ribosome rearrangement. *Cell*, **158**, 121–131.
39. Svidritskiy,E., Brilot,A.F., Koh,C.S., Grigorieff,N. and Korostelev,A.A. (2014) Structures of yeast 80S ribosome-tRNA complexes in the rotated and nonrotated conformations. *Structure*, **22**, 1210–1218.
40. Lomakin,I.B. and Steitz,T.A. (2013) The initiation of mammalian protein synthesis and mRNA scanning mechanism. *Nature*, **500**, 307–311.
41. Schilling-Bartetzko,S., Franceschi,F., Sternbach,H. and Nierhaus,K.H. (1992) Apparent association constants of tRNAs for the ribosomal A, P, and E sites. *J. Biol. Chem.*, **267**, 4693–4702.
42. Wilson,D.N. and Nierhaus,K.H. (2006) The E-site story: the importance of maintaining two tRNAs on the ribosome during protein synthesis. *Cell. Mol. Life Sci.*, **63**, 2725–2737.
43. Labuda,D., Striker,G., Grosjean,H. and Porschke,D. (1985) Mechanism of codon recognition by transfer RNA studied with oligonucleotides larger than triplets. *Nucleic. Acids Res.*, **13**, 3667–3683.